Subcell *a posteriori* limitation for DG scheme through flux recontruction

François Vilar

Institut Montpelliérain Alexander Grothendieck
Université de Montpellier

May 24th, 2018

1 Introduction

2 DG as a subcell finite volume

3 *A posteriori* subcell limitation

4 Numerical results

History

- Introduced by Reed and Hill in 1973 in the frame of the neutron transport
- Major development and improvements by B. Cockburn and C.-W. Shu in a series of seminal papers

Procedure

- Local variational formulation
- Piecewise polynomial approximation of the solution in the cells
- Choice of the numerical fluxes
- Time integration

Advantages

- Natural extension of Finite Volume method
- Excellent analytical properties (L_2 stability, $hp-$adaptivity, ...)
- Extremely high accuracy (superconvergent for scalar conservation laws)
- Compact stencil (involve only face neighboring cells)

1D scalar conservation law

- $\dfrac{\partial u}{\partial t} + \dfrac{\partial F(u)}{\partial x} = 0, \qquad (x,t) \in \omega \times [0,T]$
- $u(x,0) = u_0(x), \qquad x \in \omega$

$(k+1)^{\text{th}}$ order discretization

- $\{\omega_i\}_i$ a partition of ω, such that $\omega_i = [x_{i-\frac{1}{2}}, x_{i+\frac{1}{2}}]$
- $0 = t^0 < t^1 < \dots < t^N = T$ a partition of the temporal domain $[0,T]$
- $u_h(x,t)$ the numerical solution, such that $u_{h|\omega_i} = u_h^i \in \mathbb{P}^k(\omega_i)$

$$u_h^i(x,t) = \sum_{m=1}^{k+1} u_m^i(t)\, \sigma_m(x)$$

- $\{\sigma_m\}_m$ a basis of $\mathbb{P}^k(\omega_i)$

Variational formulation on ω_i

- $\displaystyle\int_{\omega_i} \left(\frac{\partial u}{\partial t} + \frac{\partial F(u)}{\partial x} \right) \psi \, \mathrm{d}x$ with $\psi(x)$ a test function

Integration by parts

- $\displaystyle\int_{\omega_i} \frac{\partial u}{\partial t} \psi \, \mathrm{d}x - \int_{\omega_i} F(u) \frac{\partial \psi}{\partial x} \, \mathrm{d}x + \Big[F(u)\, \psi \Big]_{x_{i-\frac{1}{2}}}^{x_{i+\frac{1}{2}}} = 0$

Approximated solution

- Substitute u by u_h^i
- Take ψ among the basis function σ_p
- $\displaystyle\sum_{m=1}^{k+1} \frac{\partial u_m^i}{\partial t} \int_{\omega_i} \sigma_m \, \sigma_p \, \mathrm{d}x = \int_{\omega_i} F(u_h^i) \frac{\partial \sigma_p}{\partial x} \, \mathrm{d}x - \Big[\mathcal{F} \, \sigma_p \Big]_{x_{i-\frac{1}{2}}}^{x_{i+\frac{1}{2}}}$

Numerical flux

- $\mathcal{F}_{i+\frac{1}{2}} = \mathcal{F}\left(u_h^i(x_{i+\frac{1}{2}}, t), u_h^{i+1}(x_{i+\frac{1}{2}}, t) \right)$
- $\mathcal{F}(u, v) = \dfrac{F(u) + F(v)}{2} - \dfrac{\gamma(u, v)}{2} (v - u)$
- $\gamma(u, v) = \max(|F'(u)|, |F'(v)|)$ Local Lax-Friedrichs

Subcell resolution of DG scheme

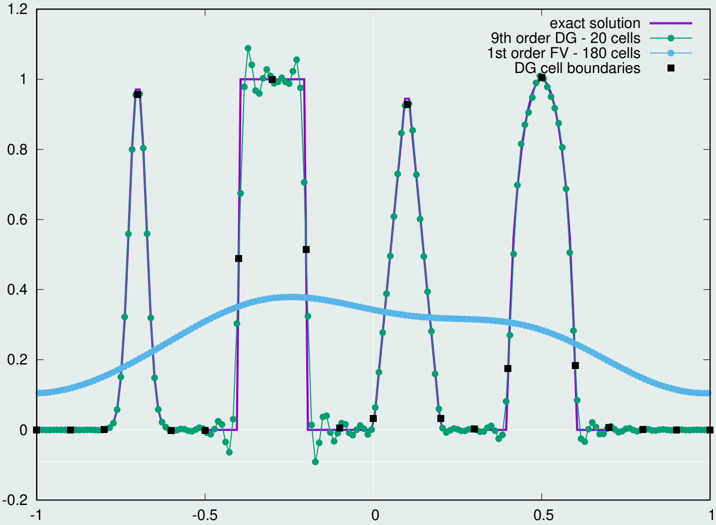

Figure : Linear advection of composite signal after 4 periods

Subcell resolution of DG scheme

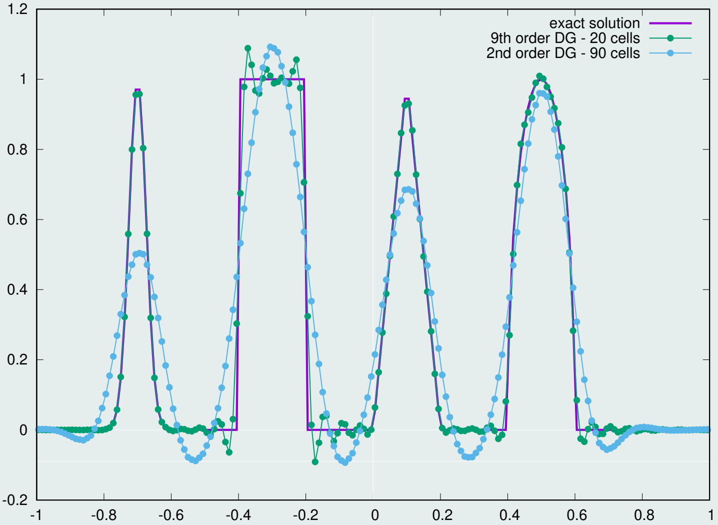

Figure : Linear advection of composite signal after 4 periods

Gibbs phenomenon

- High-order schemes leads to spurious oscillations near discontinuities
- Leads potentially to nonlinear instability, non-admissible solution, crash
- Vast literature of how prevent this phenomenon to happen:

$\Longrightarrow$ *a priori* and ***a posteriori*** limitations

A priori limitation

- Artificial viscosity
- Flux limitation
- Slope/moment limiter
- Hierarchical limiter
- ENO/WENO limiter

A posteriori limitation

- MOOD (“Multi-dimensional Optimal Order Detection”)
- Subcell finite volume limitation
- **Subcell limitation through flux reconstruction**

Admissible numerical solution

- Maximum principle / positivity preserving
- Prevent the code from crashing (for instance avoiding NaN)
- **Ensure the conservation of the scheme**

Spurious oscillations

- Discrete maximum principle
- Relaxing condition for smooth extrema

Accuracy

- Retain as much as possible the subcell resolution of the DG scheme
- Minimize the number of subcell solutions to recompute

1 Introduction

2 DG as a subcell finite volume

3 *A posteriori* subcell limitation

4 Numerical results

DG as a subcell finite volume

- Rewrite DG scheme as a specific finite volume scheme on subcells
- Exhibit the corresponding subcell numerical fluxes: **reconstructed flux**

Variational formulation

- $\displaystyle\int_{\omega_i} \frac{\partial u_h^i}{\partial t}\,\psi\,\mathrm{d}x = \int_{\omega_i} F(u_h^i)\frac{\partial \psi}{\partial x}\,\mathrm{d}x - \Big[\mathcal{F}\,\psi\Big]_{x_{i-\frac{1}{2}}}^{x_{i+\frac{1}{2}}} = 0, \qquad \forall\,\psi \in \mathbb{P}^k(\omega_i)$
- Quadrature rule exact for polynomials up to degree $2k$
- $F(u_h^i) \approx F_h^i \in \mathbb{P}^{k+1}(\omega_i)$ (collocated or projection)
- $\displaystyle\int_{\omega_i} \frac{\partial u_h^i}{\partial t}\,\psi\,\mathrm{d}x = -\int_{\omega_i} \frac{\partial F_h^i}{\partial x}\,\psi\,\mathrm{d}x + \Big[(F_h^i - \mathcal{F})\,\psi\Big]_{x_{i-\frac{1}{2}}}^{x_{i+\frac{1}{2}}}$

Subcells decomposition through $k+2$ flux points

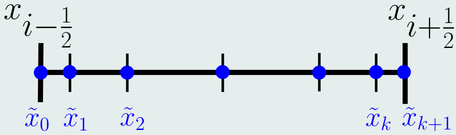

Subresolution basis functions

- ω_i is subdivided in $k+1$ subcells $S_m^i = [\widetilde{x}_{m-1}, \widetilde{x}_m]$
- Let us introduce the $k+1$ basis functions $\{\phi_m\}_m$ such that $\forall\, \psi \in \mathbb{P}^k(\omega_i)$

$$\int_{\omega_i} \phi_m \, \psi \, \mathrm{d}x = \int_{S_m^i} \psi \, \mathrm{d}x, \qquad \forall\, m = 1, \ldots, k+1$$

- $\displaystyle\sum_{m=1}^{k+1} \phi_m(x) = 1$
- Let us define $\overline{\psi}_m = \dfrac{1}{|S_m^i|} \displaystyle\int_{S_m^i} \psi \, \mathrm{d}x$ the subcell mean value

Variational formulation

- $\displaystyle\int_{\omega_i} \frac{\partial\, u_h^i}{\partial t} \, \phi_m \, \mathrm{d}x = -\int_{\omega_i} \frac{\partial\, F_h^i}{\partial x} \phi_m \, \mathrm{d}x + \Big[(F_h^i - \mathcal{F}) \, \phi_m \Big]_{x_{i-\frac{1}{2}}}^{x_{i+\frac{1}{2}}}$
- $\displaystyle |S_m^i| \frac{\partial\, \overline{u}_m^i}{\partial t} = -\int_{S_m^i} \frac{\partial\, F_h^i}{\partial x} \, \mathrm{d}x + \Big[(F_h^i - \mathcal{F}) \, \phi_m \Big]_{x_{i-\frac{1}{2}}}^{x_{i+\frac{1}{2}}}$

Subcell finite volume

- $$\frac{\partial \overline{u}_m^i}{\partial t} = -\frac{1}{|S_m^i|}\left(\left[F_h^i\right]_{\widetilde{x}_{m-1}}^{\widetilde{x}_m} - \left[\phi_m\left(F_h^i - \mathcal{F}\right)\right]_{x_{i-\frac{1}{2}}}^{x_{i+\frac{1}{2}}}\right)$$
- We introduce the $k+2$ function $L_m(x)$, the Lagrangian basis functions associated to the flux points
- Let us define $\widehat{F}_h^i = \sum_{m=0}^{k+1} \widehat{F}_m^i \, L_m(x) \in \mathbb{P}^{k+1}(\omega_i)$ such that

$$\widehat{F}_m^i - \widehat{F}_{m-1}^i = \left[F_h^i\right]_{\widetilde{x}_{m-1}}^{\widetilde{x}_m} - \left[\phi_m\left(F_h^i - \mathcal{F}\right)\right]_{x_{i-\frac{1}{2}}}^{x_{i+\frac{1}{2}}}, \qquad \forall m = 1,\dots,k+1$$

$$\widehat{F}_0^i = \mathcal{F}_{i-\frac{1}{2}} \qquad \text{and} \qquad \widehat{F}_{k+1}^i = \mathcal{F}_{i+\frac{1}{2}}$$

Reconstructed flux

- $$\widehat{F}_m^i = F_h^i(\widetilde{x}_m) - C_{i-\frac{1}{2}}^{(m)}\left(F_h^i(x_{i-\frac{1}{2}}) - \mathcal{F}_{i-\frac{1}{2}}\right) - C_{i+\frac{1}{2}}^{(m)}\left(F_h^i(x_{i+\frac{1}{2}}) - \mathcal{F}_{i+\frac{1}{2}}\right)$$
- $$C_{i-\frac{1}{2}}^{(m)} = \sum_{p=m+1}^{k+1} \phi_p(x_{i-\frac{1}{2}}) \qquad \text{and} \qquad C_{i+\frac{1}{2}}^{(m)} = \sum_{p=1}^{m} \phi_p(x_{i+\frac{1}{2}})$$

Correction terms

- Let $\boldsymbol{B} \in \mathbb{R}^{k+1}$ be defined as $\quad B_j = (-1)^{j+1} \dfrac{(k+1)(k+j)!}{(j!)^2(k+1-j)!}$
- $\widetilde{\xi}_m = \dfrac{\widetilde{x}_m - x_{i-\frac{1}{2}}}{x_{i+\frac{1}{2}} - x_{i-\frac{1}{2}}}, \quad \forall\, m = 0, \ldots, k+1$
- $C^{(m)}_{i-\frac{1}{2}} = \begin{pmatrix} 1 - (\widetilde{\xi}_m) \\ \vdots \\ 1 - (\widetilde{\xi}_m)^{k+1} \end{pmatrix} \cdot \boldsymbol{B}$ and $C^{(m)}_{i+\frac{1}{2}} = \begin{pmatrix} 1 - (1 - \widetilde{\xi}_m) \\ \vdots \\ 1 - (1 - \widetilde{\xi}_m)^{k+1} \end{pmatrix} \cdot \boldsymbol{B}$

Subcell finite volume equivalent to DG

- $\dfrac{\partial\, \overline{u}^i_m}{\partial t} = -\dfrac{1}{|S^i_m|} \left[\widehat{F}^i_h\right]^{\widetilde{x}_m}_{\widetilde{x}_{m-1}}, \qquad \forall\, m = 1, \ldots, k+1$
- Other choice on the correction terms lead to different schemes (spectral difference, spectral volume, ...)

Pointwise evolution scheme

- $\displaystyle\int_{\omega_i} \phi_m \left(\frac{\partial u_h^i}{\partial t} + \frac{\partial \widehat{F}_h^i}{\partial x}\right) \mathrm{d}x = 0, \qquad \forall\, m = 1, \dots, k+1$
- $\displaystyle\int_{\omega_i} \psi \left(\frac{\partial u_h^i}{\partial t} + \frac{\partial \widehat{F}_h^i}{\partial x}\right) \mathrm{d}x = 0, \quad \forall \psi \in \mathbb{P}^k(\omega_i) \quad \Longrightarrow \quad \frac{\partial u_h^i}{\partial t} + \frac{\partial \widehat{F}_h^i}{\partial x} = O_{\mathbb{P}^k}$

$$\forall\, m = 1, \dots, k+1, \quad \frac{\partial u_h^i(x_m, t)}{\partial t} + \frac{\partial \widehat{F}_h^i(x_m, t)}{\partial x} = 0$$

Reconstructed flux

- $\widehat{F}_h^i = F_h^i + \left(F_h^i(x_{i-\frac{1}{2}}) - \mathcal{F}_{i-\frac{1}{2}}\right) g_{LB}(x) + \left(F_h^i(x_{i+\frac{1}{2}}) - \mathcal{F}_{i+\frac{1}{2}}\right) g_{RB}(x)$
- The $g_{LB}(x)$ and $g_{RB}(x)$ are the correction functions taking into account the flux discontinuities
- To recover DG scheme, the correction functions writes

$$g_{LB}(x) = \sum_{m=0}^{k+1} C_{i-\frac{1}{2}}^{(m)} L_m(x) \qquad \text{and} \qquad g_{RB}(x) = \sum_{m=0}^{k+1} C_{i+\frac{1}{2}}^{(m)} L_m(x)$$

Reconstructed flux

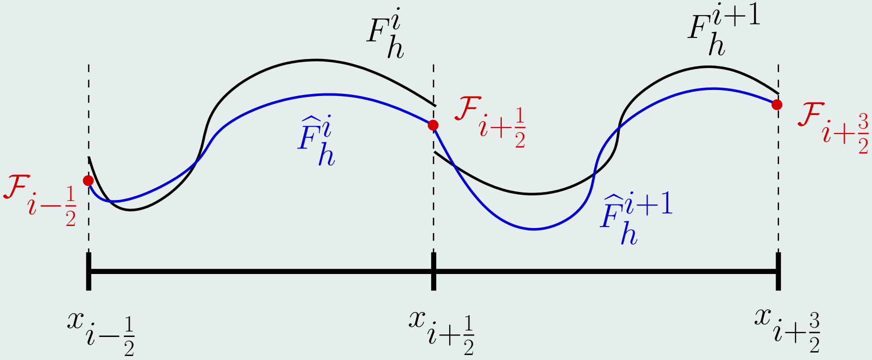

Figure : Reconstructed flux taking into account flux jumps

Flux reconstruction / CPR

- In the case of DG scheme, the correction functions $g_{LB}(x)$ and $g_{RB}(x)$ are nothing but the right and left Radau $\mathbb{P}^k$ polynomials

H. T. Huynh, *A Flux Reconstruction Approach to High-Order Schemes Including Discontinuous Galerkin Methods.* 18th AIAA Computational Fluid Dynamics Conference Miami, 2007.

Z.J. Wang and H. Gao, *A unifying lifting collocation penalty formulation including the discontinuous Galerkin, spectral volume/difference methods for conservation laws on mixed grids.* JCP, 2009.

- In the FR/CPR approach, the reconstructed flux is used pointwisely at some solution points to resolve the PDE

Subcell finite volume

- The reconstructed flux is used as a numerical flux for the subcell finite volume scheme
- The correction terms are very simple and explicitly defined
- There is no need to make use of Radau polynomial

1. Introduction
2. DG as a subcell finite volume
3. *A posteriori* subcell limitation
4. Numerical results

RKDG scheme

- SSP Runge-Kutta: convex combinations of first-order forward Euler
- For sake of clarity, we focus on forward Euler time stepping
- $u_h^{i,n}(x) = \displaystyle\sum_{m=1}^{k+1} u_m^{i,n}\,\sigma_m(x)$
- $\displaystyle\int_{\omega_i} u_h^{i,n+1}\,\sigma_p\,\mathrm{d}x = \int_{\omega_i} u_h^{i,n}\,\sigma_p\,\mathrm{d}x + \Delta t\left(\int_{\omega_i} F_h^{i,n}\frac{\partial\,\sigma_p}{\partial x}\,\mathrm{d}x - \left[\mathcal{F}^n\,\sigma_p\right]_{x_{i-\frac{1}{2}}}^{x_{i+\frac{1}{2}}}\right)$

Projection on subcells of RKDG solution

- A k^{th} degree polynomial is uniquely defined by its $k+1$ submean values
- Introducing the matrix $\mathbf{\Pi}$ defined as $\pi_{mp} = \dfrac{1}{|S_m^i|}\displaystyle\int_{S_m^i}\sigma_p\,\mathrm{d}x,$ then

$$\mathbf{\Pi}\begin{pmatrix} u_1^{i,n} \\ \vdots \\ u_{k+1}^{i,n}\end{pmatrix} = \begin{pmatrix} \overline{u}_1^{i,n} \\ \vdots \\ \overline{u}_{k+1}^{i,n}\end{pmatrix}$$

Projection

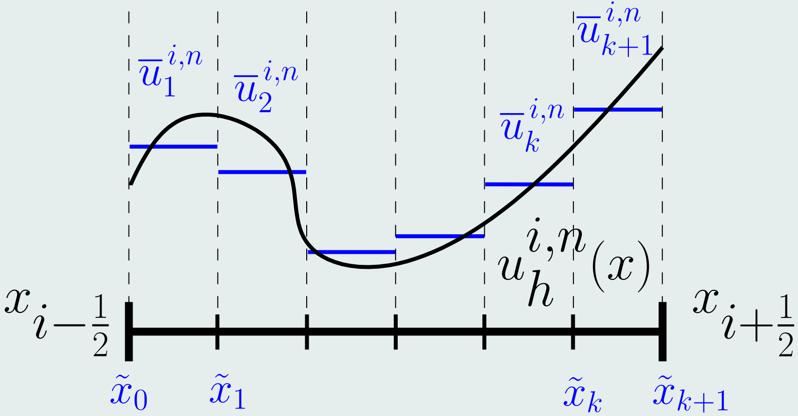

Figure : Polynomial solution and its associated submean values

Set up

- Compute a candidate solution u_h^{n+1} from u_h^n through unlimited DG
- For each cell, compute the submean values $\{\overline{u}_m^{i,n+1}\}_m$
- We assume that, for each cell, the $\{\overline{u}_m^{i,n}\}_m$ are admissible

Physical admissibility detection (PAD)

- Check if $\overline{u}_m^{i,n+1}$ lies in an convex physical admissible set (maximum principle for SCL, positivity of the pressure and density for Euler, ...)
- Check if there is any *NaN* values

Numerical admissibility detection (NAD)

- Discrete maximum principle DMP on submean values:

$$\min_p(\overline{u}_p^{i-1,n},\overline{u}_p^{i,n},\overline{u}_p^{i+1,n}) \leq \overline{u}_m^{i,n+1} \leq \max_p(\overline{u}_p^{i-1,n},\overline{u}_p^{i,n},\overline{u}_p^{i+1,n})$$

- This criterion needs to be relaxed to preserve smooth extrema

Relaxation of the DMP

- $v_L = \overline{\partial_x u}_i^{\,n+1} - \frac{\Delta x_i}{2}\,\overline{\partial_{xx} u}_i^{\,n+1}$
- $v_{\min\,\backslash\,\max} = \min\backslash\max\,(\overline{\partial_x u}_i^{\,n+1}, \overline{\partial_x u}_{i-1}^{\,n+1})$
- If $\quad (v_L > \overline{\partial_x u}_i^{\,n+1}) \quad$ Then $\quad \alpha_L = \min(1, \dfrac{v_{\max} - \overline{\partial_x u}_i^{\,n+1}}{v_R - \overline{\partial_x u}_i^{\,n+1}})$
- If $\quad (v_L < \overline{\partial_x u}_i^{\,n+1}) \quad$ Then $\quad \alpha_L = \min(1, \dfrac{v_{\min} - \overline{\partial_x u}_i^{\,n+1}}{v_R - \overline{\partial_x u}_i^{\,n+1}})$

- $v_R = \overline{\partial_x u}_i^{\,n+1} + \frac{\Delta x_i}{2}\,\overline{\partial_{xx} u}_i^{\,n+1}$
- $v_{\min\,\backslash\,\max} = \min\backslash\max\,(\overline{\partial_x u}_i^{\,n+1}, \overline{\partial_x u}_{i+1}^{\,n+1})$
- If $\quad (v_R > \overline{\partial_x u}_i^{\,n+1}) \quad$ Then $\quad \alpha_R = \min(1, \dfrac{v_{\max} - \overline{\partial_x u}_i^{\,n+1}}{v_R - \overline{\partial_x u}_i^{\,n+1}})$
- If $\quad (v_R < \overline{\partial_x u}_i^{\,n+1}) \quad$ Then $\quad \alpha_R = \min(1, \dfrac{v_{\min} - \overline{\partial_x u}_i^{\,n+1}}{v_R - \overline{\partial_x u}_i^{\,n+1}})$

Relaxation of the DMP

- $\alpha = \min(\alpha_L, \alpha_R)$
- If $(\alpha = 1)$ Then DMP is relaxed

Hierarchical limiter

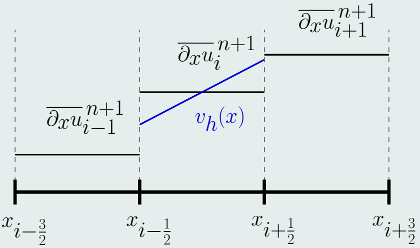

- $v_h(x) = \overline{\partial_x u}_i^{n+1} + (x - x_i)\,\overline{\partial_{xx} u}_i^{n+1}$

M. Yang and Z.J. Wang, *A parameter-free generalized moment limiter for high-order methods on unstructured grids.* AAMM., 2009.

D. Kuzmin, *A vertex-based hierarchical slope limiter for p-adaptive discontinuous Galerkin methods.* J. of Comp. and Appl. Math., 2010.

Marked subcells

- If a subcell mean value does not respect the PAD and NAD, the corresponding subcell is marked
- For all the marked subcells, as well as their first neighbors, we go back to time t^n to recompute the submean value

Corrected reconstructed flux

- $\widetilde{F}_m^i = \mathcal{F}(\overline{u}_m^{i,n}, \overline{u}_{m+1}^{i,n})$ if S_{m-1}^i or S_m^i is marked

  with $\overline{u}_0^{i,n} = \overline{u}_{k+1}^{i-1,n}$ and $\overline{u}_{k+2}^{i,n} = \overline{u}_1^{i+1,n}$
- $\widetilde{F}_m^i = \widehat{F}_m^i$ otherwise

Modified submean values

- $\overline{u}_m^{i,n+1} = \overline{u}_m^{i,n} - \dfrac{\Delta t}{|S_m^i|}(\widetilde{F}_m^i - \widetilde{F}_{m-1}^i)$
- Check if the modified submean values are now admissible
- By means of $\mathbf{\Pi}^{-1}$, get the corrected moments $\left(u_1^{i,n+1}, \dots, u_{k+1}^{i,n+1}\right)^{\mathrm{t}}$

Limited reconstructed flux

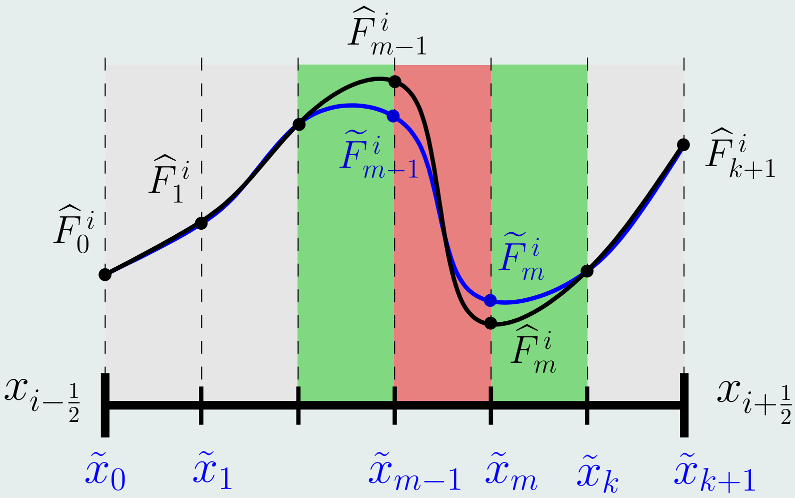

Figure : Correction of the reconstructed flux

Flowchart

1. Project $u_h^{i,n+1}$ to get the submean values $\overline{u}_m^{i,n+1}$
2. Check $\overline{u}_m^{i,n+1}$ through PAD and NAD
3. If $\overline{u}_m^{i,n+1}$ is admissible go further in time, otherwise modify the corresponding reconstructed flux values

$$\widetilde{F}^i_{m-1} = \mathcal{F}(\overline{u}^{i,n}_{m-1}, \overline{u}^{i,n}_m) \quad \text{and} \quad \widetilde{F}^i_m = \mathcal{F}(\overline{u}^{i,n}_m, \overline{u}^{i,n}_{m+1})$$

4. Through the corrected reconstructed flux, recompute the submean values for tagged subcells and their first neighbors
5. Return to point 2

Conclusion

- The limitation only affects the DG solution at the subcell scale
- The limited scheme is conservative at the subcell level
- In practice, few submean values need to be recomputed

1 Introduction

2 DG as a subcell finite volume

3 *A posteriori* subcell limitation

4 Numerical results

Initial solution on $x \in [0, 1]$

- $u_0(x) = \sin(2\pi x)$
- Periodic boundary conditions

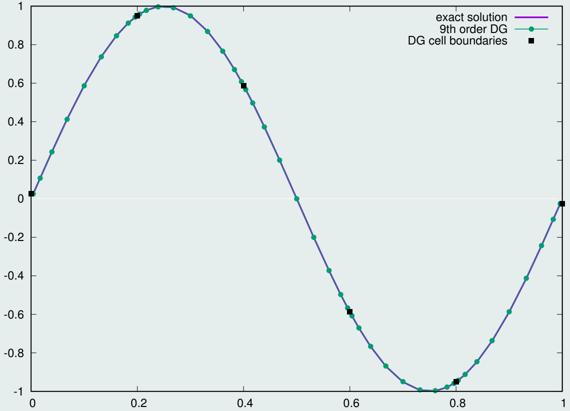

Figure : Linear advection with a 9th DG scheme and 5 cells after 1 period

Convergence rates

	L_1		L_2	
h	$E^h_{L_1}$	$q^h_{L_1}$	$E^h_{L_2}$	$q^h_{L_2}$
$\frac{1}{20}$	8.07E-11	9.00	8.97E-11	9.00
$\frac{1}{40}$	1.58E-13	9.00	1.75E-13	9.00
$\frac{1}{80}$	3.08E-16	-	3.42E-16	-

Table: Convergence rates for the linear advection case for a 9th order DG scheme

Linear advection of a square signal after 1 period

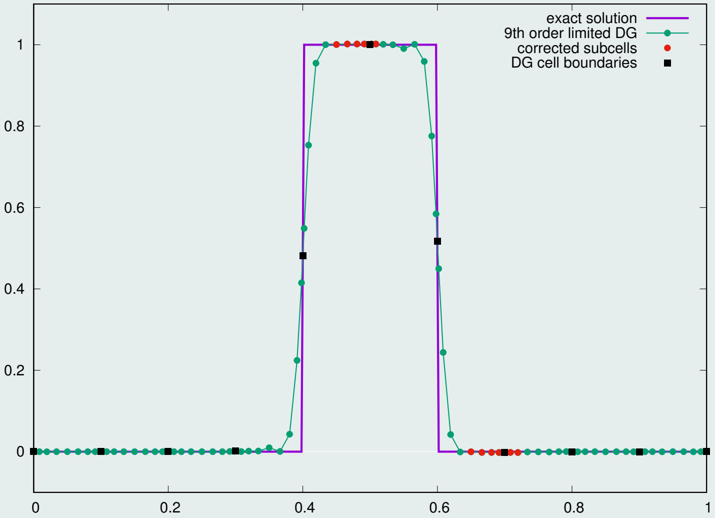

Figure : 9th order limited DG: NAD criterion

Linear advection of a square signal after 1 period

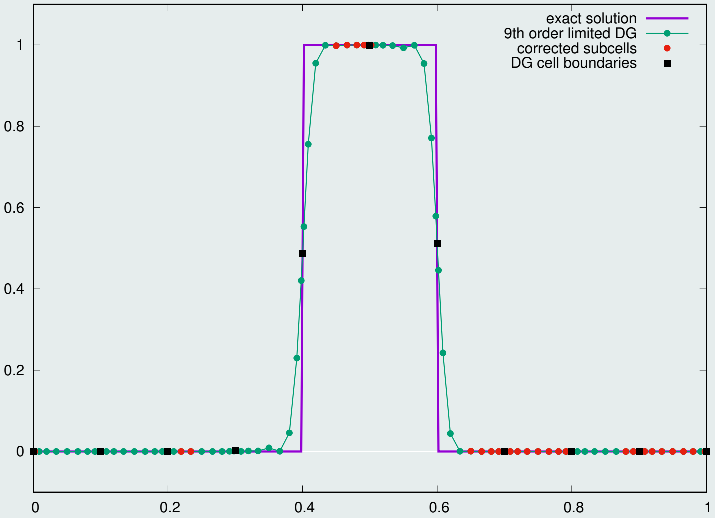

Figure : 9th order limited DG on 10 cells: NAD and PAD criteria

Linear advection of a square signal after 1 period

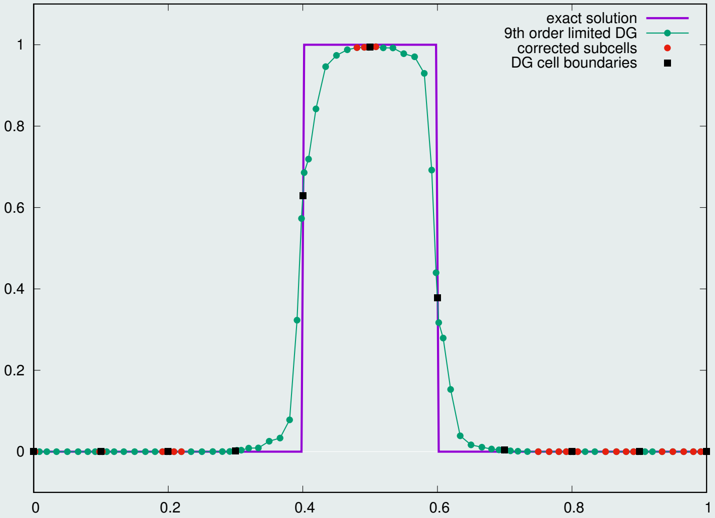

Figure : 9th order limited DG on 10 cells: subcell DMP

Linear advection of a square signal after 1 period

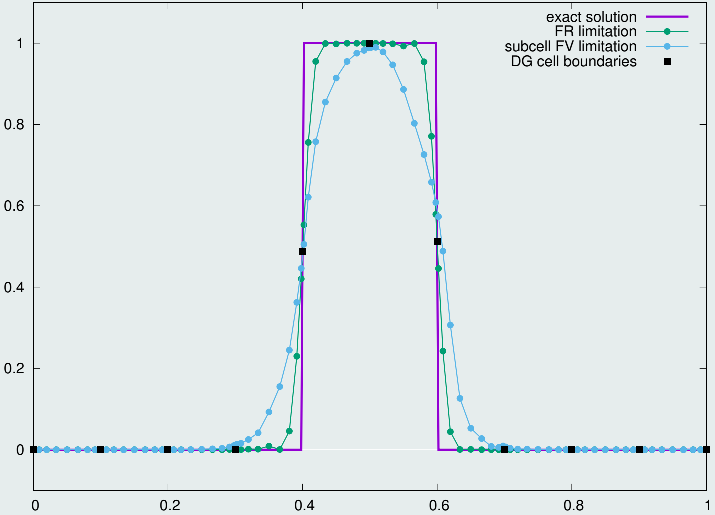

Figure : Comparison between flux reconstruction limitation and subcell finite volume limitation

Linear advection of a square signal after 10 periods

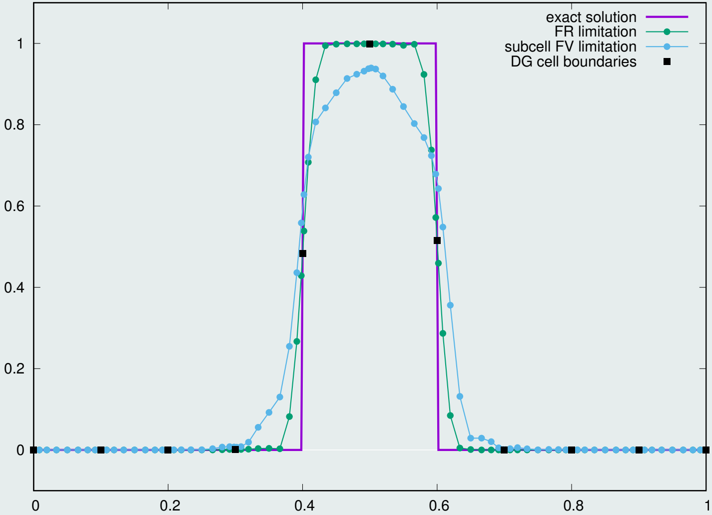

Figure : Comparison between flux reconstruction limitation and subcell finite volume limitation

Linear advection of a square signal after 50 periods

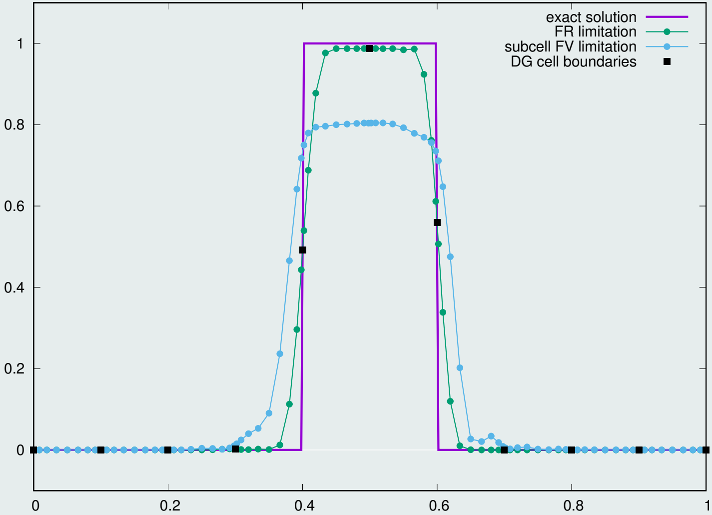

Figure : Comparison between flux reconstruction limitation and subcell finite volume limitation

Linear advection of a composite signal after 4 periods

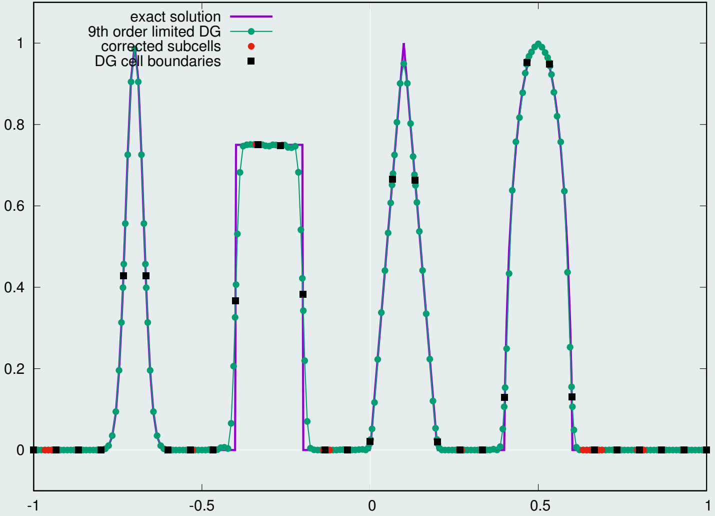

Figure : 9th order limited DG after 4 periods on 30 cells

Linear advection of a composite signal after 4 periods

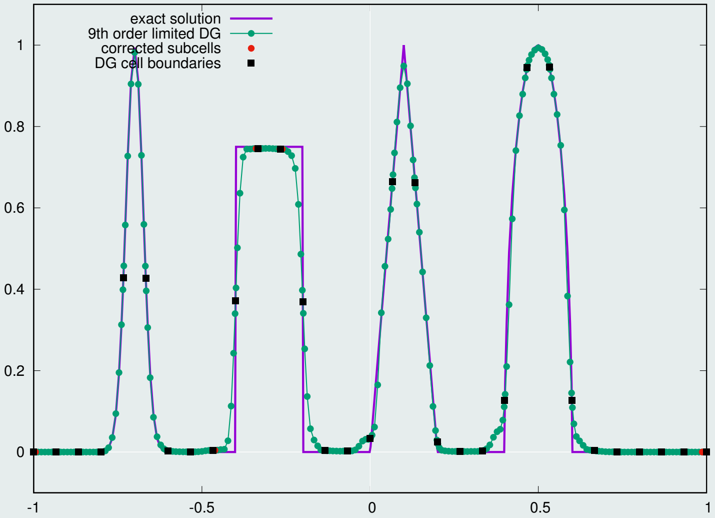

Figure : 9th order limited DG after 4 periods on 30 cells: subcell DMP

Burgers equation: $u_0(x) = \sin(2\pi\, x)$

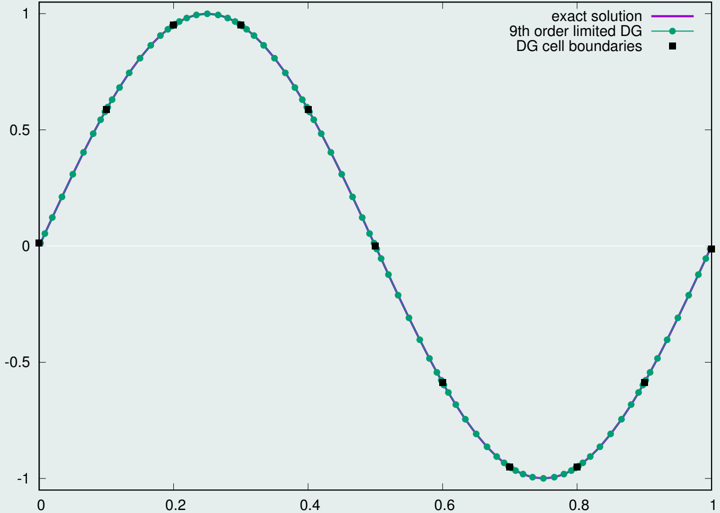

Figure : 9th order limited DG on 10 cells for $t_f = 0.7$

Burgers equation: expansion and shock waves collision

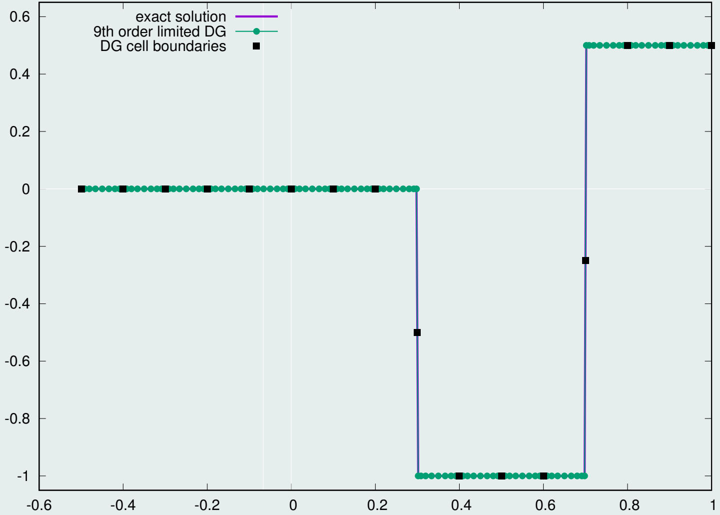

Figure : 9th order limited DG on 15 cells for $t_f = 1.2$

2D grid and subgrid

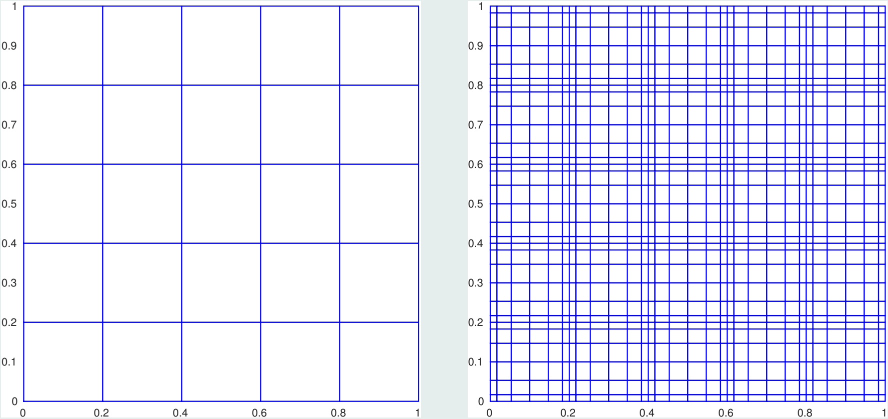

(a) Grid

(b) Subgrid

Figure : 5x5 Cartesian grid and corresponding subgrid for a 6th order DG scheme

Initial solution on $(x, y) \in [0, 1]^2$

- $u_0(x, y) = \sin(2\pi(x + y))$
- Periodic boundary conditions

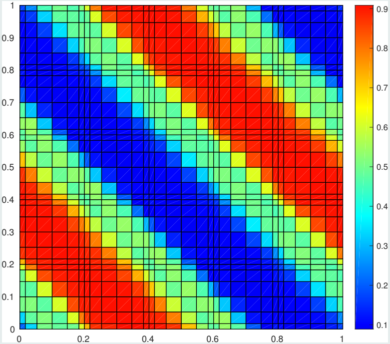

(c) Solution map

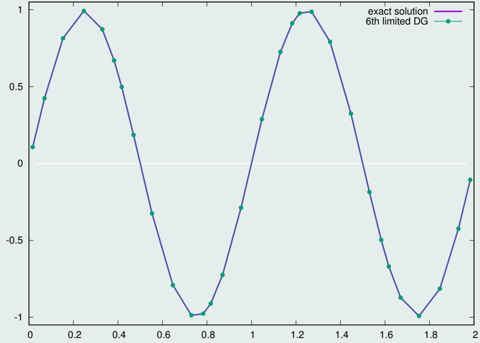

(d) Solution profile

Figure : Linear advection with a 6th DG scheme and 5x5 grid after 1 period

Convergence rates

	L_1		L_2	
h	$E^h_{L_1}$	$q^h_{L_1}$	$E^h_{L_2}$	$q^h_{L_2}$
$\frac{1}{5}$	2.10E-6	6.23	2.86E-6	6.24
$\frac{1}{10}$	2.79E-8	6.00	3.77E-8	6.00
$\frac{1}{20}$	3.36E-10	-	5.91E-10	-

Table: Convergence rates for the linear advection case for a 6th order DG scheme

Linear advection of a square signal after 1 period

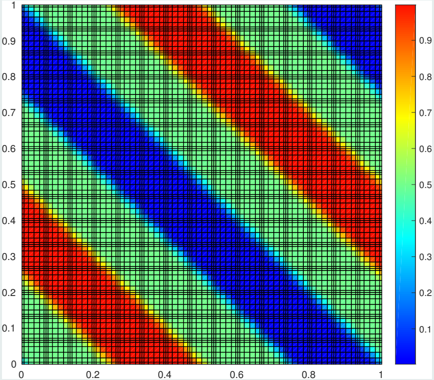

(e) Solution map

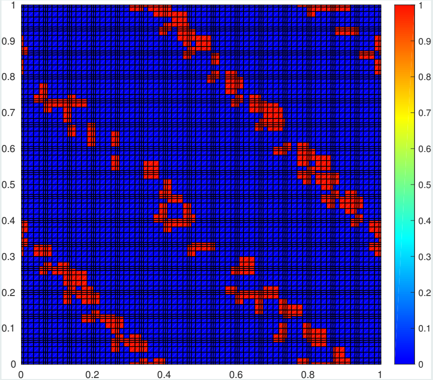

(f) Solution profile

Figure : 6th order limited DG on a 15x15 Cartesian mesh

Linear advection of a square signal after 1 period

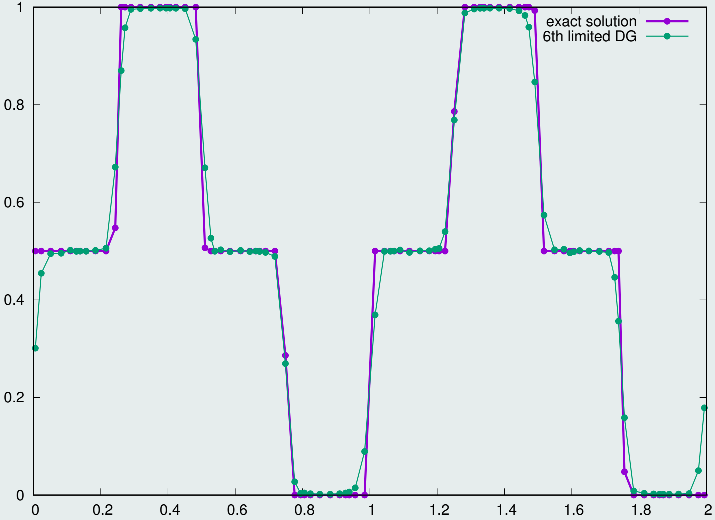

Figure : 6th order limited DG on a 15x15 Cartesian mesh

Rotation of a composite signal after 1 period

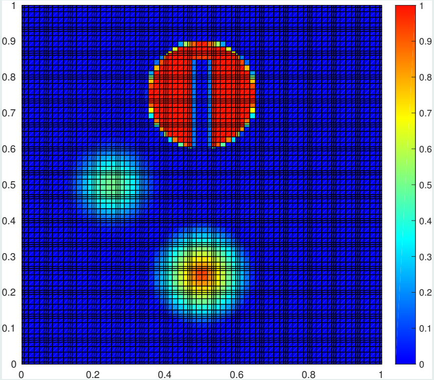

(g) Initial solution

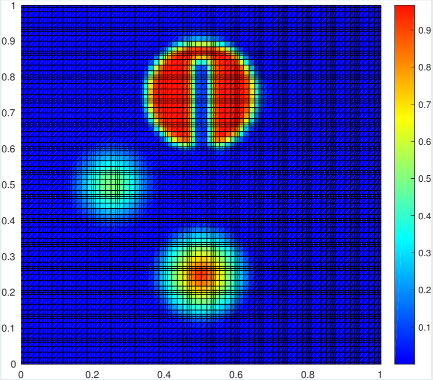

(h) Final solution

Figure : 6th order limited DG on a 15x15 Cartesian mesh

Rotation of a composite signal after 1 period

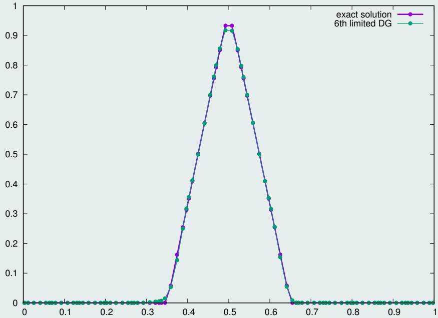

(i) Solution profile for $y = 0.25$

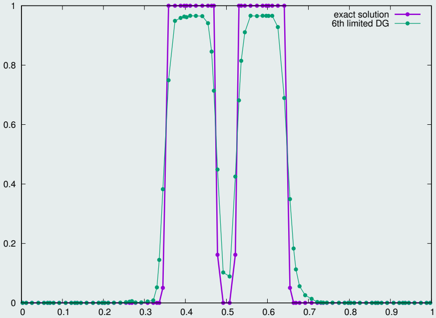

(j) Solution profile for $y = 0.75$

Figure : 6th order limited DG on a 15x15 Cartesian mesh

Rotation of a composite signal after 1 period: $x = 0.25$

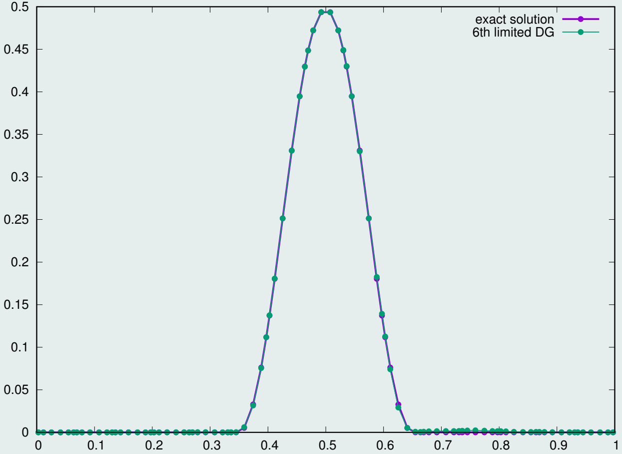

Figure : 6th order limited DG on a 15x15 Cartesian mesh

Burgers equation with $u_0(x, y) = \sin(2\pi\,(x + y))$

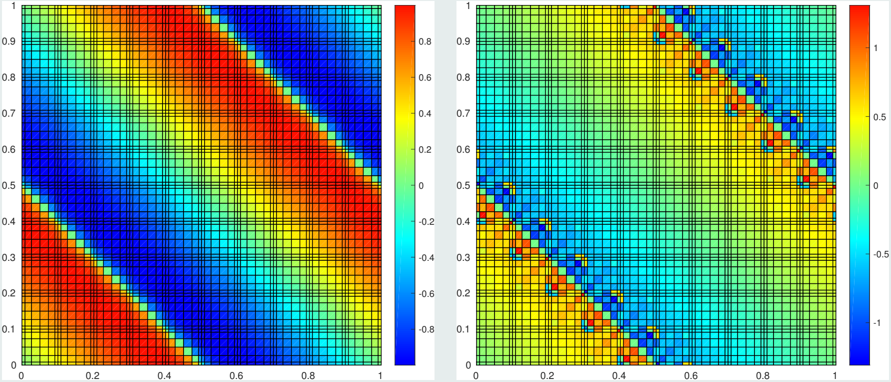

(k) Solution at $t = 0.007$ (l) Solution at $t = 0.25$

Figure : 6th order unlimited DG on a 10x10 Cartesian mesh

Burgers equation with $u_0(x, y) = \sin(2\pi\,(x + y))$

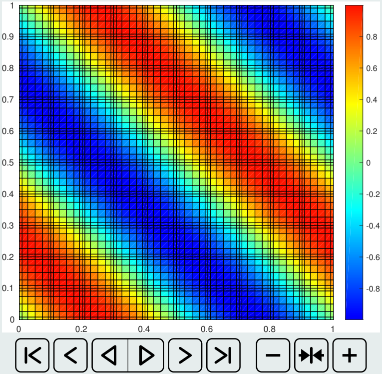

(m) Solution map

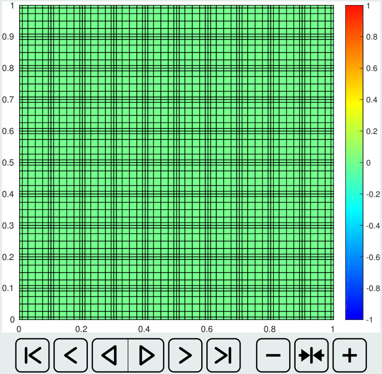

(n) Detected subcells

Figure : 6th order limited DG on a 10x10 Cartesian mesh until $t = 0.5$

Burgers equation with $u_0(x, y) = \sin(2\pi\,(x + y))$ at $t = 0.5$

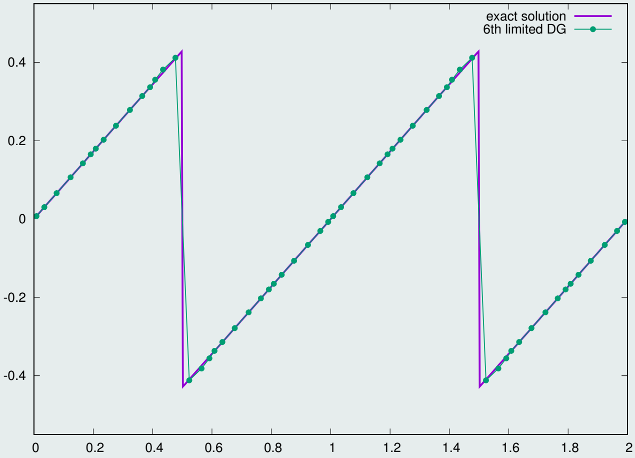

Figure : 6th order limited DG density profile on a 10x10 Cartesian mesh

Burgers equation with composite signal

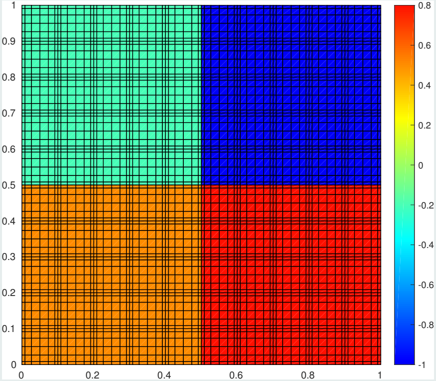

(o) Initial solution

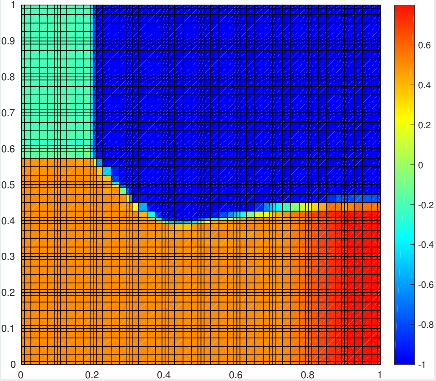

(p) Solution at $t = 0.5$

Figure : 6th order limited DG on a 10x10 Cartesian mesh

Initial solution on $x \in [0,1]$ for $\gamma = 3$

- $\rho_0(x) = 1 + 0.999999\sin(\pi x), \quad u_0(x) = 0, \quad p_0(x) = (\rho_0(x))^\gamma$
- Periodic boundary conditions

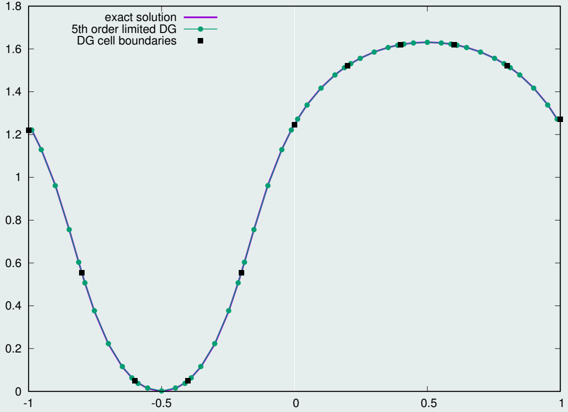

Figure : Smooth flow problem with 5th DG scheme and 10 cells at $t = 0.1$

Convergence rates

	L_1		L_2	
h	$E_{L_1}^h$	$q_{L_1}^h$	$E_{L_2}^h$	$q_{L_2}^h$
$\frac{1}{20}$	1.48E-5	4.35	2.02E-5	4.18
$\frac{1}{40}$	9.09E-7	4.88	1.38E-6	4.87
$\frac{1}{80}$	3.09E-8	4.95	4.73E-8	4.86
$\frac{1}{160}$	1.00E-9	-	1.63E-9	-

Table: Convergence rates on the pressure for the Euler equation for a 5th order DG

Sod shock tube problem

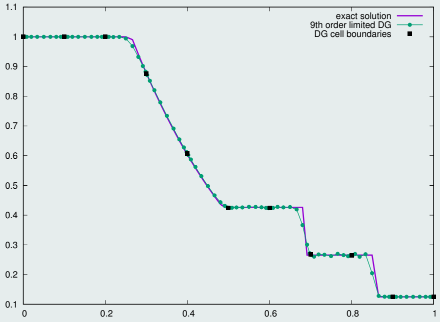

(q) PAD + NAD (r) PAD + subDMP

Figure : 9th order limited DG on 10 cells

Hell shock tube problem

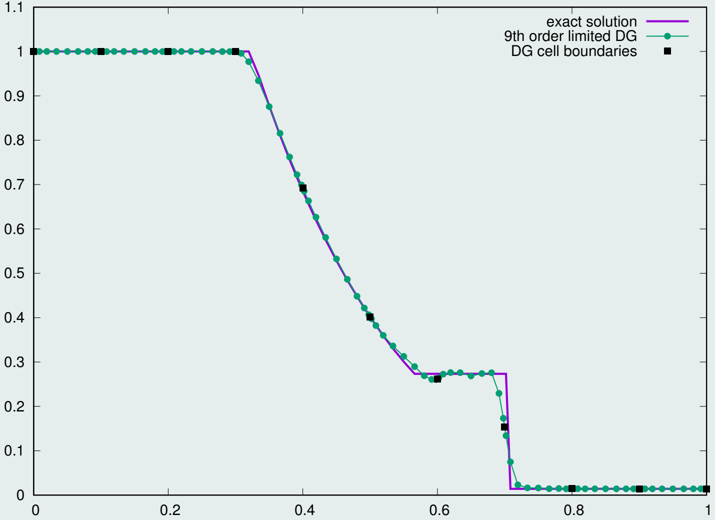

Figure : 9th order limited DG on 10 cells

Double rarefaction problem

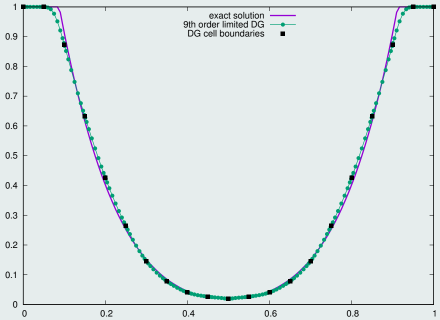

(s) Density

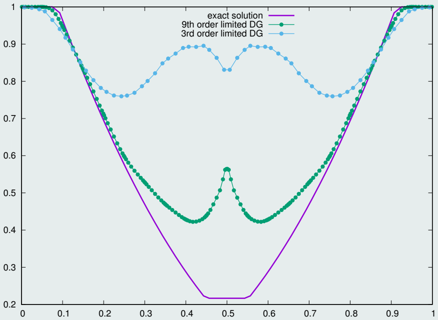

(t) Internal energy

Figure : 9th order limited DG on 20 cells

Leblanc shock tube problem

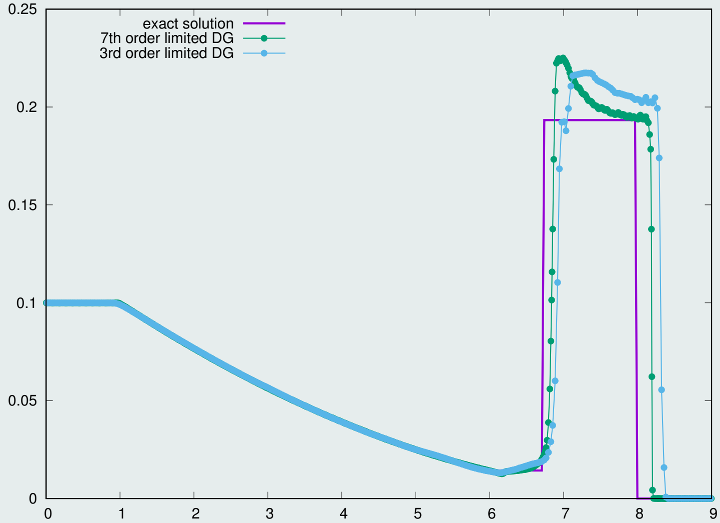

Figure : 3rd order vs 7th order limited DG on 100 cells

Shock acoustic-wave interaction problem

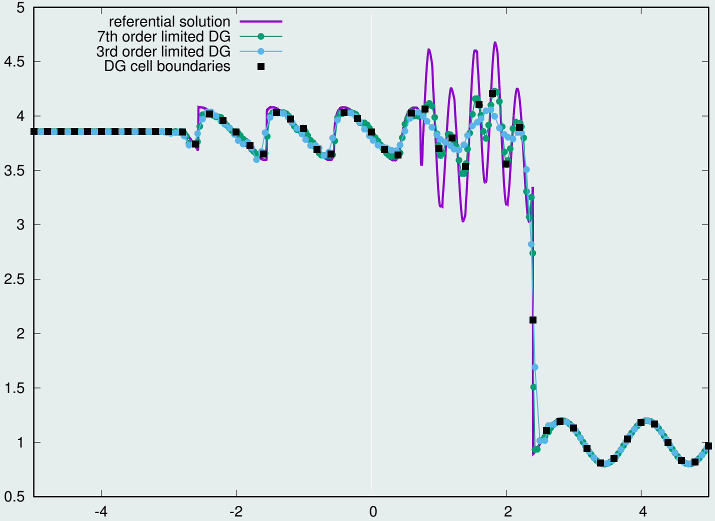

Figure : 7th order limited DG on 50 cells

Shock acoustic-wave interaction problem

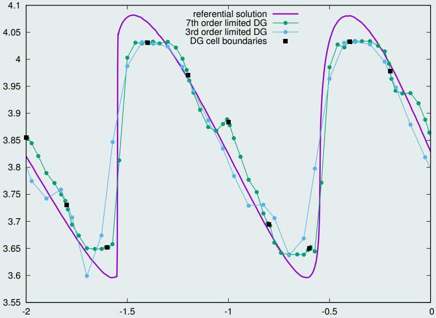

(u) Zoom on $[-2, 0]$

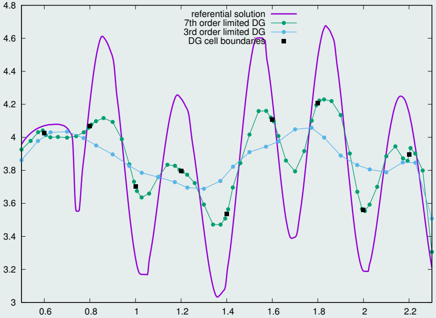

(v) Zoom on $[0.5, 2.3]$

Figure : 7th order limited DG on 50 cells

Shock acoustic-wave interaction problem

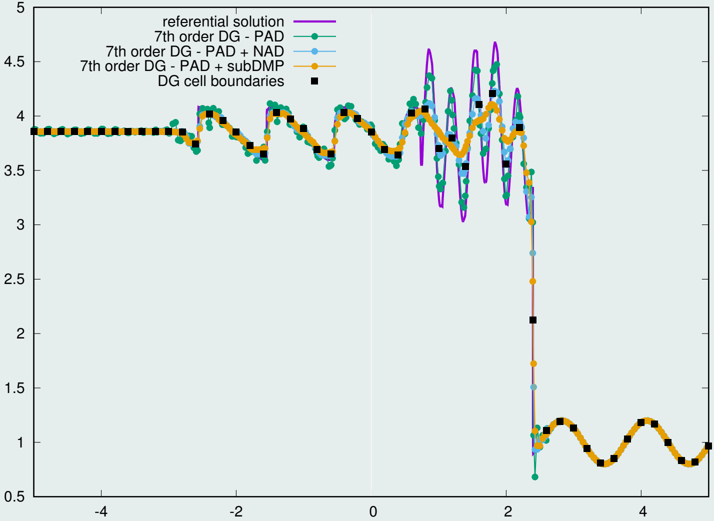

Figure : 7th order limited DG on 50 cells

Shock acoustic-wave interaction problem

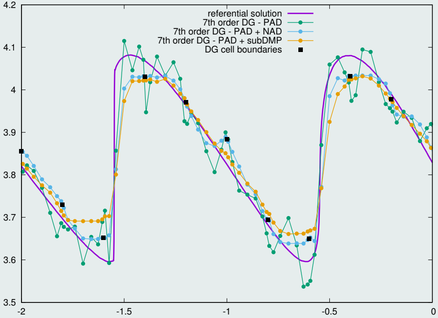

(w) Zoom on $[-2, 0]$

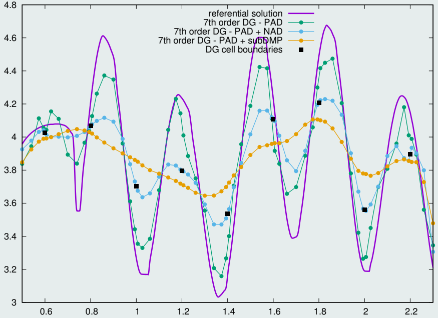

(x) Zoom on $[0.5, 2.3]$

Figure : 7th order limited DG on 50 cells